https://doi.org/10.5194/egusphere-2025-2662
Preprint. Discussion started: 3 July 2025

Identification of Micro-dynamics Phase Transition processes for Ammonium Sulfate aerosols by Two-dimensional Correlation Spectroscopy

Xiuli Wei[1,2], Xiaofeng Lu[1,2], Huaqiao Gui [1,2,3*], Jie Wang[1], Dexia Wu[1], Jianguo Liu[1,2]
1 Key Laboratory of Environmental Optics and Technology, Anhui Institute of Optics and Fine Mechanics, Hefei Institutes of Physical Science, Chinese Academy of Sciences, Hefei 230031, China
2 School of Environmental Science and Optoeclectronic Technology, University of Science and Technology of China, Hefei, 230026, China
3 Institute of Environmental Hefei Comprehensive National Science Center, Hefei 230088, China
* Correspondence: Huaqiao Gui (hqgui@aiofm.ac.cn)

Abstract

Phase transitions of particles are importance because it could influence reactive gas uptake, multiphase chemical reactions pathway, ice and polar stratospheric cloud formation. The traditional understanding assumes that phase transitions are thermodynamically equilibrium, yet this is not the case at the molecular level. Current understanding can not account for these phenomena, since the interaction with water vapor induces modifications in both the composition and local chemical microenvironment of aerosols. Our findings demonstrate that these inconsistencies can be reconciled through elucidation of the microscopic dynamic processes governing phase transformation for aerosol. We propose a novel method which is accurate in determining the phase transition point and identification of micro-dynamics phase transition processes for ammonium sulfate aerosols by using two-dimensional correlation spectroscopy. During efflorescence transition processes, we measured the phase transition point at 39% ± 0.8% (RH), and its start and end points at 41%± 0.8% (RH) and 36%± 0.8% (RH), respectively. We also explore that there are four distinct micro-dynamics steps during the efflorescence processes. Initially, there was a gradual loss of liquid water for the solution droplets. Subsequently, it formed the supersaturated ammonium sulfate (AS) particles. Furthermore, hydrogen bonds between liquid water and sulfate dissociate, reducing liquid sulfate concentration. Sulfate and ammonium ions in the bulk phase gradually approach each other, further expelling residual water. The efflorescence occurs and forms crystal/solid AS. Eventually, the remaining liquid water molecules eventually detach from the AS system, completing the liquid-to-solid phase transition. This method will help improve

https://doi.org/10.5194/egusphere-2025-2662
Preprint. Discussion started: 3 July 2025

comprehending of the transport and deposition of inhaled aerosol. Moreover these insights will spur fundamental research into the formation and transformation mechanisms of atmospheric aerosols.

Keywords:

phase transitions

micro-dynamics mechanism

efflorescence processes

supersaturated ammonium sulfate

Introduction

The phase state of aerosols governs their physical, chemical, and optical properties, thereby exerting significant impacts on the environment, climate system, and human health(Shiraiwa et al., 2017) (Meng et al., 2024), (Poschl, 2005) . It alters the phase of temperature changes in addition to the effects of relative humidity and particle size effects.(Martin, 2000; Shiraiwa et al., 2017),(Xie et al., 2017). Phase transitions of aerosol could affect reactive gas uptake, multiphase chemical reactions pathway, ice and polar stratospheric cloud formation (Martin, 2000).

It has long been assumed that aerosol phase transition behaviors are thermodynamic equilibrium and may be achieved in a short amount of time. For example, the deliquescence of particulate matter. The particle should take up some amount of water to establish thermodynamic equilibrium upon increasing humidity. Currently, the phase transition behaviors of aerosol have been extensively investigated by a diversity of methods. For example, the environmental scanning electron microscope (ESEM)(Treuel, Pederzani, & Zellner, 2009), the hygroscopic tandem differential mobility analyzer (H-TDMA)(Gao, Chen, & Yu, 2006), the electrodynamic balance (EDB)(Cohen, Flagan, & Seinfeld, 1987), and microresonator mass sensor(Zielinski et al., 2018). These methods can diagnosis the phase transition processes of particles by measuring the particle size, shape and other physical parameters. they have been recognized as some main parameters during the phase transition processes of aerosol particles(Cheng, Su, Koop, Mikhailov, & Poschl, 2015; Gao et al., 2006).

On molecular level, the phase transition processes are not thermodynamic equilibrium, since molecular-scale dynamics inherently deviate from thermodynamic

https://doi.org/10.5194/egusphere-2025-2662
Preprint. Discussion started: 3 July 2025

equilibrium conditions. The interaction with water vapor induces modifications in both the composition and local chemical microenvironment of aerosols. But conventional Fourier transform infrared (FTIR) spectroscopy lacks the capability to observe these transformations and quantify the water uptake and evaporation kinetics of ambient aerosol. Moreover, the overlapped and time resolution restrict its development to be a certain range in the hygroscopic or nucleation property of aerosols. In order to study the complicated physical or chemical transition processes of aerosol, two-dimensional correlation infrared spectroscopy (2D-IR) has been used (Wei et al., 2022), (Chen, Teng, Qian, & Yu, 2019).

In contrast, the molecular-scale dynamical processes governing aerosol phase transitions remain hitherto uncharacterized due to the difficulty in measuring the intermolecular interaction of the efflorescence transition processes. This is very much necessary to realize the homogeneous nucleation of atmospheric aerosol. So a precision determination methodology was developed to track complex spectral changes and analysis the micro-dynamics phase transition mechanism of aerosol. During the efflorescence transition processes, we examine the intermolecular interactions and identify phase change points and keep an eye on complicated spectrum changes by coupling a relative humidity (RH) controlling system and 2D-IR. This study could provide critical insight about redefining atmospheric heterogeneous chemistry.

1. Instruments and Methods

1.1 The samples and measurement System

Samples: In this study, all aerosol samples were generated from Ammonium Sulfate (AS) solution using an aerosol generator. The concentration of AS solution was 4.0 g/L.

The experiment system: The experiment system mainly includes a humidification system and an in situ FTIR system which has been described in ACP (Wei et al., 2022). The phase transition processes of the aerosol were measured by transmission FTIR spectroscopy (Tensor 27, Bruker Optics, Germany). One end of the sample cell is provided with a radius of 3 cm zinc selenide (ZnSe) substrate and the other end is the same ZnSe substrate containing aerosol samples. The spectral resolution is 4 cm^{-1} and a repeat time of 1 scan. The humidification system is used to provide a certain RH for the aerosol samples. It consists of dry and humidified N_2. The humidified N_2 was supplied by the high purity water vapour. By adjusting the volumetric ratio between these two N_2 streams, we could obtain a specific RH. Its accuracy is ± 0.8 % for a 0 ～

https://doi.org/10.5194/egusphere-2025-2662
Preprint. Discussion started: 3 July 2025

100 % RH range, and its time resolution is about 30 second. The AS aerosols were humidified or dehumidified at a rate of 1% min^{-1} within the range of 20% to 90% (RH). In this study, the aerosol samples with electrical mobility diameter about 300 nm were deposited on ZnSe substrate.

1.2 The two-dimensional correlation infrared spectroscopy analysis method

1.2.1 Generalized two-dimensional infrared (2D-IR) correlation spectroscopy

The two-dimensional (2D) correlation spectral function can be represented as follows:

$$X(\nu_1, \nu_2) = < \tilde{y}(\nu_1, t) \cdot \tilde{y}(\nu_2, t) > = \Phi(\nu_1, \nu_2) + i\Psi(\nu_1, \nu_2)$$

Here, $\tilde{y}$ represents a set of the dynamic spectra that are functions of both spectral variables (ν_1 and ν_2, corresponding to the spectral wavenumber of compounds the vibrations wavenumbers) and the external perturbation variable (relative humidity, RH). The synchronous ($\Phi(\nu_1, \nu_2)$) and asynchronous ($\Psi(\nu_1, \nu_2)$) correlation intensities, corresponding respectively to the real and imaginary components of the complex cross-correlation function, quantitatively describe the coordinated and sequential changes in spectral intensities at wavenumbers ν_1 and ν_2 (Chen et al., 2019; Isao Noda & Ozaki, 2014). In this study, we use the synchronous correlation maps to diagnose if the spectral intensities at different wavenumbers vary simultaneously, and the asynchronous correlation maps are use to identify the occurrence sequential order of the intermolecular interactions. In the synchronous correlation maps, the positive and negative correlations indicate simultaneous and opposite changes of the spectral intensities observed at the wavenumber pair (ν_1, ν_2), respectively. In asynchronous correlation map, positive cross-peaks suggest that spectral intensity variations at frequency ν_1 precede those at ν_2, whereas negative cross-peaks imply the inverse temporal sequence, with changes at ν_2 leading those at ν_1.

1.2.2 Perturbation-correlation moving window two-dimensional (PCMW2D) correlation infrared spectroscopy

PCMW2D correlation infrared spectroscopy serves as a powerful tool for recognizing characteristic spectral variation along the perturbation variable axis(Isao Noda, 2025; I. Noda, Park, & Jung, 2025), (Morita, Shinzawa H Fau - Noda, Noda I Fau - Ozaki, & Ozaki, 2006). This technique generates complementary synchronous and asynchronous 2D correlation spectra, visualized as contour maps with spectral variables (e.g., wavenumber) plotted against perturbation parameters (e.g., relative

https://doi.org/10.5194/egusphere-2025-2662
Preprint. Discussion started: 3 July 2025

humidity), enabling precise identification of transition points and critical regions. Consequently, PCMW2D proves particularly valuable for elucidating complex environmental processes through its distinctive analytical capabilities. In the resulting 2D-IR spectra, red-colored regions indicate positive correlation intensities, whereas blue-colored regions denote negative correlation intensities. Within synchronous correlation maps, these positive and negative correlations correspond to enhanced and diminished spectral intensity variations along the perturbation gradient, respectively. The asynchronous spectra reveal more nuanced behavior: positive correlations signify convex spectral intensity profiles along the perturbation axis, while negative correlations indicate concave profiles. Specifically, positive asynchronous correlation intensities manifest as convex curvature in RH-dependent FTIR spectral variations, with negative intensities conversely reflecting concave variation patterns.

To obtain a credible result, linear baseline corrections and smooth were performed in the regions of 1000–1500cm^{-1} and 2500–3550cm^{-1} for all infrared spectra before calculations and the analysis. These regions almost cover the absorption features of all identifiable functional groups of interest are selected for analysis. Then we normalize all pre-processed infrared spectra into 2D-IR spectra developed by Kwansei-Gakuin University, Japan (Isao Noda & Ozaki, 2014).

2. Results and discussion

In this study, the spectra were collected with a 1% (RH) at intervals. For liquid water, crystal/solid AS, and aqueous AS, their infrared absorption peaks are mainly observed in 3550-2500 cm-1 and 1500-1000 cm-1 regions (Onasch et al., 1999; Wei et al., 2022), (Juan J. Nájera, Percival, & Horn, 2009), (Miñambres, Sánchez, Castaño, & Basterretxea, 2010). For clarity, the spectra and the detailed assignments of the infrared spectra bands are listed in table 1.

Table 1. The detailed infrared spectra bands assignments of AS aerosol appearing in RH-dependent FTIR

Compounds state	species	Peak position Wavenumber/cm^{-1}	Ref
liquid water	O-H stretching	3600-3100	(Onasch et al., 1999; Schlenker & Martin, 2005), (Cai, Luan, Shi, & Zhang, 2017)
Crystal/solid AS	NH_4^+ deformation	~ 1417	(Onasch et al.,

https://doi.org/10.5194/egusphere-2025-2662
Preprint. Discussion started: 3 July 2025

	(ν4-NH_4^+)		1999), (Juan J. Nájera et al., 2009), (Miñambres et al., 2010), (Zhu, Pang, & Zhang, 2022)
	SO_4^{2-} stretching	~ 1112, ~ 1083	
aqueous AS	NH_4^+ deformation (ν4-NH_4^+)	~ 1463	(Juan J. Nájera et al., 2009), (Miñambres et al., 2010)
	SO_4^{2-} stretching	~ 1097	

2.1 Humidity-dependent FTIR spectra of AS aerosols upon efflorescence

In Fig. 1(A) shows the RH-dependent FTIR spectra of AS in 3600-2550 cm^{-1} region upon efflorescence. The intensities of the stretching vibration of O–H groups at ~3400 cm^{-1} decrease and its wavenumber does not red or blue shift during the whole efflorescence processes. When RH decreased from 90% to 80%, the intensities of the stretching vibration of O–H groups at ~3400 cm^{-1} decrease. It can be deduced that it is a gradual loss of liquid water for the AS solution droplets upon efflorescence. When RH (from 80% to 41%) decreases below the efflorescence point, the intensities of the stretching vibration of O–H groups at ~3400 cm^{-1} continue decrease, while aqueous AS droplets undergo persistent water evaporation and become AS supersaturated state. The intensities decrease at ~3400 cm^{-1} will terminate when RH decreased from 41% to 36%. It means all condensed-phase water is driven and the hydration networks breakdown. AS aerosol would change to fully crystal/solid state at 36% (RH). It indicates the efflorescence phase transition of AS aerosol would be from liquid to supersaturated state, ultimately reaching crystal/solid phase.

https://doi.org/10.5194/egusphere-2025-2662
Preprint. Discussion started: 3 July 2025

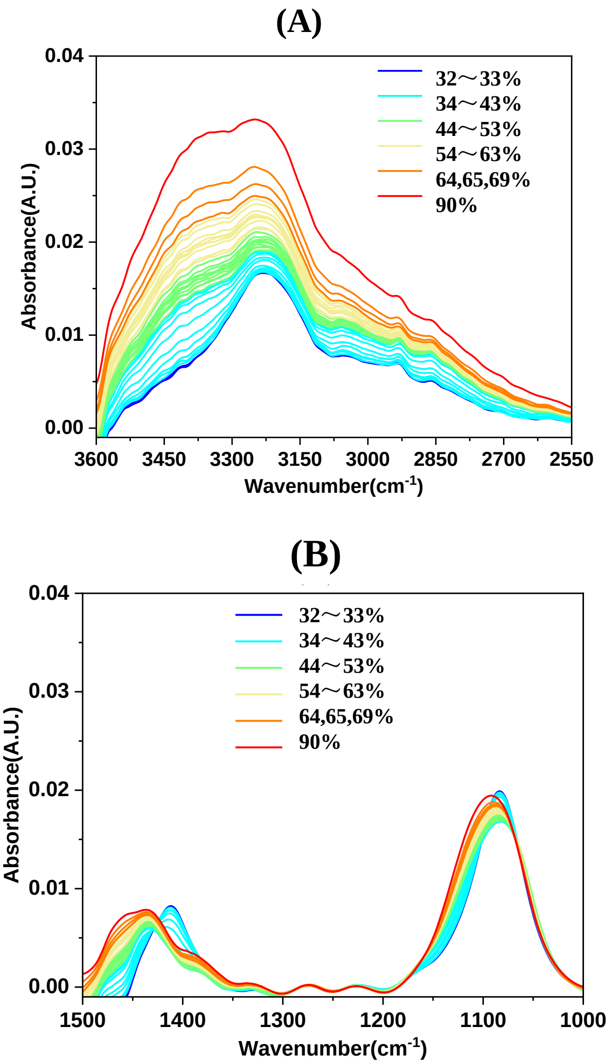

Fig.1 Humidity-dependent FTIR spectra of AS particles upon efflorescence from 65% to 32 at a rate of 1%RH. (A) 3600-2550cm^{-1}; (B) 1500-1000cm^{-1}.

SO_4^{2-} acts as a "structure maker" due to its tetrahedral configuration, facilitating hydrogen bond formation with surrounding water molecules. Similarly, NH_4^+ contributes to water structure stabilization through its tetrahedral geometry and hydrogen bonding capacity (Dong et al., 2007). Based on the shifting of the SO_4^{2-} and NH_4^+ mode in the FTIR spectra as a result of the phase transformation. In Fig. 1(B) shows the RH-dependent FTIR spectra of AS in 1500-1000 cm^{-1} region upon efflorescence. The ν_3-SO_4^{2-} bands at 1097 cm^{-1} and 1084 cm^{-1} correspond to the

https://doi.org/10.5194/egusphere-2025-2662
Preprint. Discussion started: 3 July 2025

aqueous and crystal/solid state, respectively. And the ν_4-NH_4^+ bands at 1463 cm^{-1} and 1417 cm^{-1} correspond to the aqueous and crystal/solid state, respectively. As relative humidity (RH) decreased from 90% to 42%, both of the intensities at 1094 cm^{-1} and 1463 cm^{-1} gradually diminished, indicating progressive water loss from the droplet solution. When RH decreased from 41% to 36%, a distinct phase transition occurred between 41% and 36% (RH), characterized by an abrupt shift in the ν_4-NH_4^+ peak position from 1463 cm^{-1} to 1417 cm^{-1}, accompanied by a sharp intensity increase, signaling the onset of anhydrous crystal formation. The same trend has been observed with sulfate, namely: an abrupt shift in the ν_3-SO_4^{2-} peak position from 1097 cm^{-1} to 1084 cm-1, accompanied by a sharp intensity increase. Complete crystallization was achieved at 36% (RH) when the intensities at 1084 cm^{-1} and 1417 cm-1 were constant. So the crystallization threshold of AS was identified at 41% (RH) and completed at 36%(RH), consistent with prior studies (Cai et al., 2017; Cziczo & Abbatt, 1999; J. J. Nájera & Horn, 2009). Comparable behavior was observed in the O-H stretching vibration modes, where absorption peak intensities exhibited analogous humidity-dependent variations for ammonium and sulfate ions in aqueous AS also gradually decrease. But these absorption peaks of ammonium and sulfate ions do not disappear but instead exhibit a red shift(Zhu et al., 2022). The reason is that when the AS transitions from liquid to crystal/solid state, the surrounding environment of the ammonium and sulfate ions change.

2.2 PCMW2D Correlation Analysis of AS aerosols upon efflorescence

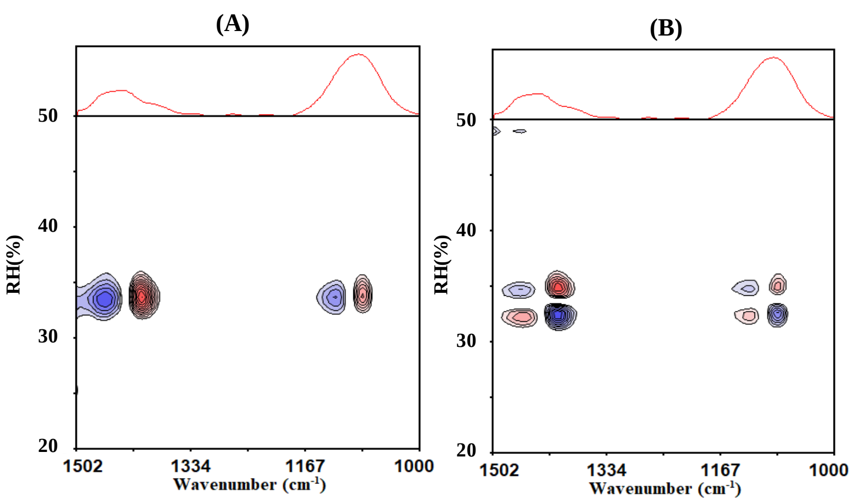

https://doi.org/10.5194/egusphere-2025-2662
Preprint. Discussion started: 3 July 2025

Synchronous Asynchronous

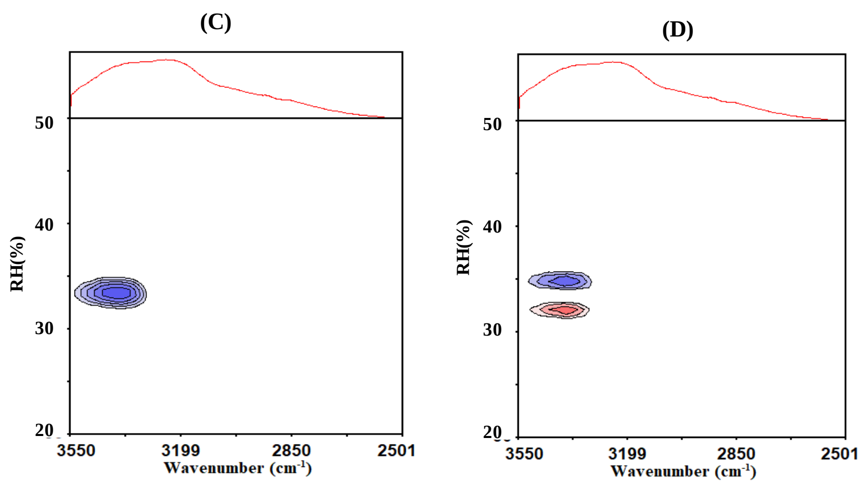

Synchronous Asynchronous

Fig.2 (A)Synchronous and (B)asynchronous PCMW2D spectra in the 1502-1000 cm^{-1} region during the efflorescence process of AS aerosol; (C)Synchronous and (D)asynchronous PCMW2D spectra in the 3550-2501 cm^{-1} region during the efflorescence process of AS aerosol. Red and blue means a positive and negative correlation value, respectively.

To accurately determine the exact DRH of AS, we further analysis the PCMW2D spectra. Fig.2(A) gives the synchronous PCMW2D spectra in 1502-1000 cm^{-1} region during the efflorescence process of AS aerosol. As can be seen, (1084 cm^{-1}, 39%) and (1417 cm^{-1}, 39%) show red color, which is a positive correlation peak, indicating that crystal/solid sulfate and ammonium ions concentration increased at 39%(RH). While (1097 cm^{-1}, 39%) and (1463 cm^{-1}, 39%) are negative correlation peaks, indicating that liquid sulfate and ammonium ions concentration diminished. Combined with one-dimensional FTIR spectroscopy, the hydrogen bonds for SO_4^{2-} with water molecules and NH_4^+ ions with water molecules are dramatically disrupted. So liquid sulfate and ammonium ions changed to crystal/solid sulfate and ammonium at 39% (RH). This means the efflorescence phase transition point is 39%± 0.8% (RH). It is consistent with the findings of Takahama et al. (2007)(Takahama, Pathak, & Pandis, 2007), Yeung et al. (2009) (Yeung, Lee, & Chan, 2009), who measured the deliquescence point of AS at 38 ~ 40%(Xu, Imre, McGraw, & Tang, 1998). Therefore, this method can be used to analyze the aerosol phase change process.

Fig.2(B) is the same as (A) but the asynchronous PCMW2D spectra. (1084cm^{-1},

https://doi.org/10.5194/egusphere-2025-2662
Preprint. Discussion started: 3 July 2025

41%) shows red as a positive correlation peak, and (1084cm^{-1}, 36%) shows blue as a negative correlation peak. It demonstrated that the 1084 cm^{-1} band intensity rose convexly and concavely by 41% and 36%, respectively. Notably, the asynchronous correlation at 1084 cm^{-1} shifted from positive to negative (implying a linear increase) at approximately 39% (RH). This suggests a sharpened intensification of the 1084 cm^{-1} band near the 39% (RH). (1097cm^{-1}, 36%) showed red, which was a positive correlation peak, and (1097cm^{-1}, 41%) showed blue, which was a negative correlation peak. It indicated the 1097 cm^{-1} band intensity concavely and convexly decreases at 41% and 36%. (1417cm^{-1}, 41%) showed red, which was a positive correlation peak, and (1417cm^{-1}, 36%) showed blue, which was a negative correlation peak. (1463cm^{-1}, 36%) showed red, which was a positive correlation, and (1463cm^{-1}, 41%) showed blue, which was a negative correlation. Therefore, we can infer that 39% is the maximum phase transition point for supersaturated AS, while 41% and 36% correspond to the initial and termination points of the change of its liquid to the crystal/solid state, respectively.

In order to clearly analyze the variation of infrared absorption peaks at 1084 cm^{-1}, 1097 cm^{-1}, 1417 cm^{-1} and 1463 cm^{-1}, we listed the two-dimensional correlated infrared absorption peaks in Figure 2 and gave them in Table 2. Positive and negative values of the infrared absorption peaks in the two-dimensional correlated infrared synchronous and asynchronous spectra, and the variation of the absorption peaks inferred according to the PCMW2D reading rules. Liquid sulfate and ammonium ion concentration convex decrement at 41%, linear decrement 39%, at last concave decrement at 36%. And the crystal/solid sulfate and ammonium show the opposite trend.

Table 2. The positions and symbols of the peaks, the transition RH determined upon efflorescence from Fig. 2

https://doi.org/10.5194/egusphere-2025-2662
Preprint. Discussion started: 3 July 2025

Synchronous	Asynchronous	Spectra change	
(1084cm^{-1}, 39%) +	(1084cm^{-1}, 36%)-		41 39 36
	(1084cm^{-1}, 41%) +		
(1097cm^{-1}, 39%) -	(1097cm^{-1}, 36%) +		41 39 36
	(1097cm^{-1}, 41%) -		
(1417cm^{-1}, 39%) +	(1417cm^{-1}, 36%) -		41 39 36
	(1417cm^{-1}, 41%) +		
(1463cm^{-1}, 39%) -	(1463cm^{-1}, 36%) +		41 39 36
	(1463cm^{-1}, 41%) -		

Fig.2(C) and (D) are the same as (A) and (B) but in the region of 3550-2501cm^{-1}. From the synchronous correlation spectrum, it can be seen that (3400 cm^{-1}, 39%) appears red, which is a positive correlation peak. From the asynchronous correlation spectrum, it can be seen that (3400 cm^{-1}, 41%) and (3400cm^{-1}, 36%) appears blue and red, respectively. there is a negative and positive correlation peak, respectively. Therefore, we can infer that the efflorescence phase transition point was 39%. The liquid AS began to lose water at 41%, and crystallization occurred at 39%. At last, AS particles completely turned into crystal/solid state and the condensed water has completely disappeared at 36%.

Therefore AS is in a supersaturated state when RH is above 41%(Dong et al., 2007). With the humidity reduction from 41% to 36%, the liquid water molecules around the liquid sulfate ions and ammonium ions begin to precipitate slowly, occurs obvious efflorescence at 39% (RH), when the humidity is reduced to 36%, the liquid water molecules around the sulfate ions are completely replaced by ammonium ions, and the AS particles change from liquid state to crystal/solid state, so the efflorescence phase transformation process completed.

2.3 Generalized 2D-IR correlation spectra analysis of AS aerosols upon efflorescence

https://doi.org/10.5194/egusphere-2025-2662
Preprint. Discussion started: 3 July 2025

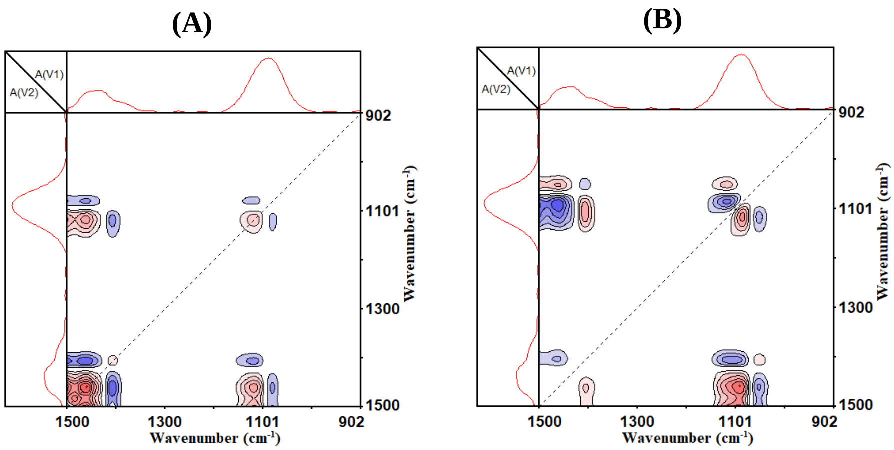

Synchronous Asynchronous

Fig. 3(A) synchronous and (B) asynchronous 2D-IR correlation spectra of AS aerosol in the 1500-902 cm-1 region upon efflorescence. Red and blue color represent positive and negative correlations, respectively. RH ranges is 90～20% (RH), red and blue means a positive and negative correlation value, respectively.

Fig.3 shows the generalized 2D-IR correlation spectra of AS particles upon efflorescence. In the synchronous 2D-IR correlation spectra, four strong auto-peaks are observed at (1097, 1463) cm^{-1}, (1417, 1463) cm^{-1}, (1097, 1417) cm^{-1}, and (1084, 1463) cm^{-1}, indicating significant changes in these infrared absorption bands during the efflorescence phase transition. The positive cross-peak at (1097, 1463) cm^{-1} indicates that the absorbance variations at these wavenumbers exhibit consistent directional trends - i.e., crystal/solid sulfate (SO_4^{2-}) and ammonium (NH_4^+) increase simultaneously, while liquid sulfate and liquid ammonium decrease. Conversely, three negative cross-peaks - (1417, 1463) cm^{-1}, (1097, 1417) cm^{-1}, and (1084, 1463) cm^{-1}, which mean that the absorbance variations at these wavenumbers are oppositely directed. This implies that liquid water content in AS aerosol decreases, water molecules surrounding sulfate and ammonium ions are progressively lost, causing these ions to move closer together. Consequently, their IR absorption bands undergo red shifts from 1097 cm^{-1} to 1084 cm^{-1} and 1463 cm^{-1} to 1417 cm^{-1}. So liquid sulfate and ammonium would change to crystal/solid sulfate and ammonium. It would result in the increase of crystal/solid sulfate and ammonium concentrations upon efflorescence.

In the asynchronous 2D-IR correlation spectra, seven strong auto-peaks are present. Among them: (1417, 1463) cm^{-1}, (1097, 1463) cm^{-1}, (1084, 1417) cm^{-1}, and (1097, 1084) cm^{-1} exhibit positive auto-peaks. While (1097, 1417) cm^{-1}, (1084, 1463) cm^{-1}, and (1084, 1097) cm^{-1} show negative auto-peaks. Since asynchronous spectra reflect differing rates of spectral changes, the sequence of molecular bond transformations during efflorescence can be deduced as: (1084 cm^{-1}) > (1097 cm^{-1}) > (1463 cm^{-1}) > (1417 cm^{-1}) (where ">" denotes that the preceding band changes before the subsequent one).

By correlating the absorption band positions of SO_4^{2-} and NH_4^+ in different states with the 2D-IR transition sequence, we infer that the increase in crystal/solid sulfate and decrease in liquid sulfate do not occur simultaneously. Instead, the efflorescence mechanism processes in two main distinct steps: at initial stage, crystal/solid sulfate concentration rises as liquid water is lost from the supersaturated AS particles. Then at secondary stage, hydrogen bonds between liquid water and sulfate dissociate, reducing liquid sulfate concentration. Sulfate and ammonium ions in the bulk phase gradually approach each other, further expelling residual water. Eventually, efflorescence occurs completely, forming crystal/solid AS. Further, Combined the sequence changes upon efflorescence we conclude that NH_4^+ ions are rich around the AS surface(Tian, Byrnes, Han, & Shen, 2011).

2.4 The micro-dynamic mechanism during efflorescence process

The two-dimensional correlation infrared spectroscopy results further confirm at the molecular level that the microscopic dynamics during the phase transition process of AS particulates. During the efflorescence process, the formation of crystal/solid sulfate initiates the AS efflorescence mechanism. Specifically, the crystal/solid sulfate undergoes an increase pattern of first slow, then fast, and finally slow again, while the liquid sulfate particles exhibit a decrease pattern of first fast, then slow, and then fast again. Following this, the crystal/solid ammonium ions experience a similar slow-fast-slow increase trend, while the liquid ammonium ions decrease. Eventually, the liquid water completely detaches from the particles, resulting in the formation of crystal/solid ammonium sulfate. This phenomenon occurs because, in aerosol solutions, anions tend to accumulate more readily on the particle surface(Chamberlayne & Zare, 2020). Thus, as humidity decreases, the reduction of liquid water concentration around the surface sulfate ions leads to the formation of crystal/solid sulfate

https://doi.org/10.5194/egusphere-2025-2662
Preprint. Discussion started: 3 July 2025

Based on the two-dimensional correlation infrared spectroscopy (2D-COS) analysis of ammonium sulfate (AS) fine particles, the microscopic kinetic evolution during the efflorescence phase transition of AS particles was elucidated at the molecular level. The complete microscopic kinetic mechanism of sulfate (SO_4^{2-}) and ammonium (NH_4^+) ions is illustrated in Figure 4.

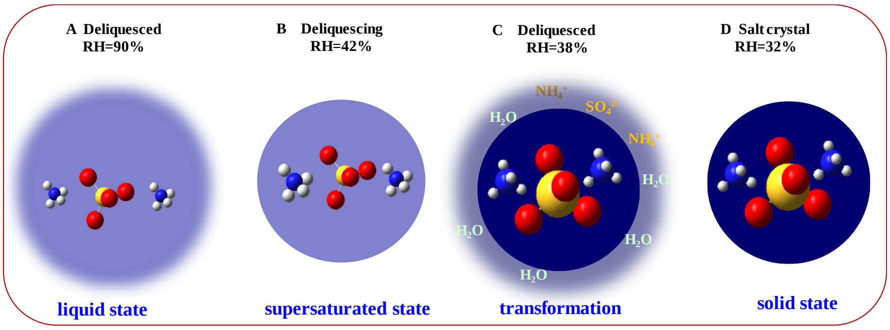

Fig 4 Schematic view of the micro-dynamic mechanism during efflorescence process

Initially, the supersaturated liquid surface of AS fine particles loses water molecules(Dong et al., 2007), leading to the formation of crystal/solid sulfate ions, which triggers the AS phase transition. This occurs because sulfate anions preferentially accumulate at the droplet surface. Subsequently, as more water molecules surrounding liquid-phase sulfate ions are gradually lost, the sulfate ions transition into the crystal/solid phase, accompanied by a gradual blue shift in the sulfate absorption peak. Concurrently, water molecules surrounding liquid-phase ammonium ions in the bulk phase are also progressively lost, allowing NH_4^+ ions to migrate closer to SO_4^{2-}, ultimately forming crystal/solid AS. As humidity further decreases, the remaining liquid water molecules eventually detach from the AS system, completing the liquid-to-solid phase transition. Thus, the entire transformation process from liquid AS to crystal/solid AS is driven by sequential dehydration, ion reconfiguration, and crystallization.

3. Conclusions

In this work, a precision determination methodology was developed to analysis the phase transition mechanism of particles by coupling a RH controlling system and 2D-IR. We measure the phase transition efflorescence point at 39% ± 0.8% (RH). Which confirms that this method is accurate in determining the phase transition point.

By correlating the absorption band positions of sulfate in different states with the 2D-COS-derived transition sequence, we infer that the increase in crystal/solid

https://doi.org/10.5194/egusphere-2025-2662
Preprint. Discussion started: 3 July 2025

sulfate and decrease in liquid sulfate do not occur simultaneously. Instead, the efflorescence mechanism divided in four steps：(1) at initial stage (RH: from 90% to 80%)：when RH decreased from 90% to 80%, the intensities of these peaks decrease. It can be deduced that this tendence upon efflorescence can be explained by a gradual loss of liquid water for the solution droplets. (2) at second stage (RH: from 80% to 41%)： When RH decreased from 80% to 41%, aqueous AS droplets undergo persistent water evaporation and become AS supersaturated state. (3) at third stage (RH: from 41% to 39%). When RH decreased from 41% to 35%, as more water molecules surrounding from the supersaturated AS particles surface are gradually lost, the sulfate ions transition into the crystal/solid phase, accompanied by a gradual blue shift in the sulfate absorption peak. hydrogen bonds between liquid water and sulfate dissociate, reducing liquid sulfate concentration. Sulfate and ammonium ions in the bulk phase gradually approach each other, further expelling residual water. Eventually, efflorescence occurs completely, forming crystal/solid AS. Concurrently, water molecules surrounding liquid-phase ammonium ions in the bulk phase are also progressively lost, allowing NH_4^+ ions to migrate closer to SO_4^{2-}, ultimately forming crystal/solid AS. (4) at last stage (RH: from 39% to 36%): As humidity further decreases, the remaining liquid water molecules eventually detach from the AS system, completing the liquid-to-solid phase transition. Thus, the entire transformation process from liquid AS to crystal/solid AS is driven by sequential dehydration, ion reconfiguration, and crystallization.

While the efflorescence properties in this study are consistent with earlier reports, the application of 2D-IR spectroscopy has enabled the elucidation of more sophisticated structural evolution patterns and the precise sequence of hydrogen-bonding rearrangements among NH_4^+, SO_4^{2-}, and H_2O. These findings deepen the mechanistic understanding of aerosol phase transitions at the molecular scale, which could advance predictive models for inhaled particle behavior. Additionally, the distinct bonding characteristics observed in AS droplets may inspire new research directions in atmospheric heterogeneous chemistry.

Author contributions.

XW designed the experiment, carried out the data analysis and wrote the paper with contributions from all co-authors; HG contributed to scientific discussions; XL contributed to this work by providing formal analysis, JW, DW and JL contributed to this work by providing constructive comments.

Competing interests

The contact author has declared that none of the authors has any competing interests.

Disclaimer

Publisher's note: Copernicus Publications remains neutral with regard to jurisdictional claims made in the text, published maps, institutional affiliations, or any other geographical representation in this paper. While Copernicus Publications makes every effort to include appropriate place names, the final responsibility lies with the authors

Acknowledgments

This work was financially supported by the National Natural Science Foundation of China (Nos. U2133212, 42375124), National Key Research and Development Program of China (No.2023YFC3705405), the Natural Science Foundation of Anhui Province (No. 2108085MD139).

References

Cai, C., Luan, Y.-m., Shi, X.-m., & Zhang, Y.-h. (2017). (NH4)2SO4 heterogeneous nucleation and glycerol evaporation of (NH4)2SO4-glycerol system in its dynamic efflorescence process. *Chemical Physics, 483-484*, 140-148. doi:https://doi.org/10.1016/j.chemphys.2016.12.003

Chamberlayne, C. F., & Zare, R. N. (2020). Simple model for the electric field and spatial distribution of ions in a microdroplet. *J Chem Phys, 152*(18), 184702. doi:10.1063/5.0006550

Chen, W., Teng, C. Y., Qian, C., & Yu, H. Q. (2019). Characterizing Properties and Environmental Behaviors of Dissolved Organic Matter Using Two-Dimensional Correlation Spectroscopic Analysis. *Environ Sci Technol, 53*(9), 4683-4694. doi:10.1021/acs.est.9b01103

Cheng, Y., Su, H., Koop, T., Mikhailov, E., & Poschl, U. (2015). Size dependence of phase transitions in aerosol nanoparticles. *Nat Commun, 6*, 5923. doi:10.1038/ncomms6923

Cohen, M. D., Flagan, R. C., & Seinfeld, J. H. (1987). Studies of concentrated electrolyte solutions using the electrodynamic balance. 1. Water activities for single-electrolyte solutions. *The Journal of Physical Chemistry, 91*(17), 4563-4574. doi:10.1021/j100301a029

Cziczo, D. J., & Abbatt, J. P. D. (1999). Deliquescence, efflorescence, and supercooling of ammonium sulfate aerosols at low temperature: Implications for cirrus cloud formation and aerosol phase in the atmosphere. *JOURNAL OF GEOPHYSICAL RESEARCH-ATMOSPHERES, 104*(D11), 13781-13790. doi:10.1029/1999JD900112

Dong, J. L., Li, X. H., Zhao, L. J., Xiao, H. S., Wang, F., Guo, X., & Zhang, Y. H. (2007). Raman observation of the interactions between NH4+, SO4(2-), and H2O in supersaturated (NH4)2SO4 droplets. *J Phys Chem B, 111*(42), 12170-12176. doi:10.1021/jp072772o

Gao, Y., Chen, S. B., & Yu, L. E. (2006). Efflorescence Relative Humidity for Ammonium Sulfate Particles. *The Journal of Physical Chemistry A, 110*(24), 7602-7608. doi:10.1021/jp057574g

Martin, S. T. (2000). Phase Transitions of Aqueous Atmospheric Particles. *Chemical Reviews, 100*(9), 3403-3454. doi:10.1021/cr990034t

Meng, X., Wu, Z., Chen, J., Qiu, Y., Zong, T., Song, M., . . . Hu, M. (2024). Particle phase state and aerosol liquid water greatly impact secondary aerosol formation: insights into phase transition and its role in haze events. *ATMOSPHERIC CHEMISTRY AND PHYSICS, 24*(4), 2399-2414. doi:10.5194/acp-24-2399-2024

Miñambres, L., Sánchez, M. N., Castaño, F., & Basterretxea, F. J. (2010). Hygroscopic Properties of Internally Mixed Particles of Ammonium Sulfate and Succinic Acid Studied by Infrared Spectroscopy. *The Journal of Physical Chemistry A, 114*(20), 6124-6130. doi:10.1021/jp101149k

Morita, S., Shinzawa H Fau - Noda, I., Noda I Fau - Ozaki, Y., & Ozaki, Y. (2006). Perturbation-correlation moving-window two-dimensional correlation spectroscopy. *Appl Spectrosc, 60*(4), 398-406. doi:10.1366/000370206776593690

Nájera, J. J., & Horn, A. B. (2009). Infrared spectroscopic study of the effect of oleic acid on the deliquescence behaviour of ammonium sulfate aerosol particles. *Physical Chemistry Chemical Physics, 11*(3), 483-494. doi:10.1039/b812182f

Nájera, J. J., Percival, C. J., & Horn, A. B. (2009). Infrared spectroscopic studies of the heterogeneous reaction of ozone with dry maleic and fumaric acid aerosol particles. *Physical Chemistry Chemical Physics, 11*(40), 9093-9103. doi:10.1039/B909623J

Noda, I. (2025). Non-Isothermal Melt Crystallization of a Biodegradable Polymer Studied by Two-Dimensional Infrared Correlation Spectroscopy. *Molecules, 30*(5). doi:10.3390/molecules30051131

Noda, I., & Ozaki, Y. (2014). Two-Dimensional Correlation Spectroscopy – Applications in Vibrational and Optical Spectroscopy. In (pp. 15-38): John Wiley & Sons.

Noda, I., Park, Y., & Jung, Y. M. (2025). Correlation Filters to Streamline Analysis of Congested Spectral Datasets. *APPLIED SPECTROSCOPY*. doi:10.1177/00037028251320106

Onasch, T. B., Siefert, R. L., Brooks, S. D., Prenni, A. J., Murray, B., Wilson, M. A., & Tolbert, M. A. (1999). Infrared spectroscopic study of the deliquescence and efflorescence of ammonium sulfate aerosol as a function of temperature. *Journal of Geophysical Research: Atmospheres, 104*(D17), 21317-21326. doi:10.1029/1999jd900384

Poschl, U. (2005). Atmospheric aerosols: composition, transformation, climate and health effects. *Angew Chem Int Ed Engl, 44*(46), 7520-7540. doi:10.1002/anie.200501122

Schlenker, J. C., & Martin, S. T. (2005). Crystallization Pathways of Sulfate−Nitrate−Ammonium Aerosol Particles. *The Journal of Physical Chemistry A, 109*(44), 9980-9985. doi:10.1021/jp052973x

Shiraiwa, M., Li, Y., Tsimpidi, A. P., Karydis, V. A., Berkemeier, T., Pandis, S. N., . . . Poschl, U. (2017). Global distribution of particle phase state in atmospheric secondary organic aerosols. *Nat Commun, 8*, 15002. doi:10.1038/ncomms15002

Takahama, S., Pathak, R. K., & Pandis, S. N. (2007). Efflorescence Transitions of Ammonium Sulfate Particles Coated with Secondary Organic Aerosol. *Environmental Science & Technology, 41*(7), 2289-2295. doi:10.1021/es0619915

Tian, C., Byrnes, S. J., Han, H.-L., & Shen, Y. R. (2011). Surface Propensities of Atmospherically

Relevant Ions in Salt Solutions Revealed by Phase-Sensitive Sum Frequency Vibrational Spectroscopy. *The Journal of Physical Chemistry Letters, 2*(15), 1946-1949. doi:10.1021/jz200791c

Treuel, L., Pederzani, S., & Zellner, R. (2009). Deliquescence behaviour and crystallisation of ternary ammonium sulfate/dicarboxylic acid/water aerosols. *Physical Chemistry Chemical Physics, 11*(36), 7976-7984. doi:10.1039/B905007H

Wei, X., Dai, H., Gui, H., Zhang, J., Cheng, Y., Wang, J., . . . Liu, J. (2022). Technical note: Real-time diagnosis of the hygroscopic growth micro-dynamics of nanoparticles with Fourier transform infrared spectroscopy. *ATMOSPHERIC CHEMISTRY AND PHYSICS, 22*(5), 3097-3109. doi:10.5194/acp-22-3097-2022

Xu, J., Imre, D., McGraw, R., & Tang, I. (1998). Ammonium Sulfate: Equilibrium and Metastability Phase Diagrams from 40 to −50 °C. *The Journal of Physical Chemistry B, 102*(38), 7462-7469. doi:10.1021/jp981929x

Yeung, M. C., Lee, A. K. Y., & Chan, C. K. (2009). Phase Transition and Hygroscopic Properties of Internally Mixed Ammonium Sulfate and Adipic Acid (AS-AA) Particles by Optical Microscopic Imaging and Raman Spectroscopy. *Aerosol Science and Technology, 43*(5), 387-399. doi:10.1080/02786820802672904

Zhu, Y., Pang, S., & Zhang, Y. (2022). Observations on the unique phase transitions of inorganics relevant due to gluconic acid in particles. *ATMOSPHERIC ENVIRONMENT, 288*, 119313. doi:https://doi.org/10.1016/j.atmosenv.2022.119313

Zielinski, A. T., Gallimore, P. J., Griffiths, P. T., Jones, R. L., Seshia, A. A., & Kalberer, M. (2018). Measuring Aerosol Phase Changes and Hygroscopicity with a Microresonator Mass Sensor. *Anal Chem, 90*(16), 9716-9724. doi:10.1021/acs.analchem.8b00114

Xie Z.B.; Gui H.Q.; Zhang J.S.; Yang B.; Kang S.P., Wei X.L.; Yu T.Z.;, Yang Y.X.; Liu J.G.; Liu W.Q., Measurement techniques new progress of atmospheric fine particles[J]. Energy Environmental Protection, 2023, 37(2): 16-29.